Electrochimica Acta 82 (2012) 12–18

Contents lists available at SciVerse ScienceDirect

Electrochimica Acta

journal homepage: www.elsevier.com/locate/electacta

Voltammetric studies of hexachromic anion transfer reactions across micro-water/polyvinylchloride-2-nitrophenyloctylether gel interfaces for sensing applications

Md. Mokarrom Hossain [a], Sang Hyuk Lee [a], Hubert H. Girault [b], Valérie Devaud [b], Hye Jin Lee [a,*]

[a] Department of Chemistry and Green-Nano Materials Research Center, Kyungpook National University, 1370 Sankyuk-dong, Buk-gu, Daegu 702-701, Republic of Korea
[b] Laboratoire d'Electrochimie Physique et Analytique, Station 6, Ecole Polytechnique Fédérale de Lausanne, CH-1015 Lausanne, Switzerland

ARTICLE INFO

Article history:
Received 2 December 2011
Received in revised form 22 March 2012
Accepted 24 March 2012
Available online 4 April 2012

Keywords:
Micro-liquid/gel interface
Amperometric sensors
Chromium(VI)
Facilitated ion transfer
Aliquat 336

ABSTRACT

The transfer reactions of various anionic hexavalent chromium species across a polarized water/polyvinylchloride-2-nitrophenyloctylether (PVC-NPOE) interface featuring a 66 microhole array are described for the development of selective and sensitive Cr(VI) sensors. The transfer of hydrophilic hexachromic anions across a liquid/liquid interface typically involves setting the potential window in a negative region. Therefore, a highly hydrophobic tetraoctylammonium tetrakis(pentafluorophenyl)borate (TOATB) salt was synthesized and incorporated into the PVC-NPOE gel phase as an organic supporting electrolyte to provide a larger potential window at the negative end. The transfer of different hexachromic anions across the microhole array interface between the aqueous and PVC-NPOE gel phase containing TOATB was first characterized by voltammetric measurements. Since Cr(VI) ion species can hold different anionic forms such as $Cr_2O_7^{2-}$, $HCrO_4^-$, and CrO_4^{2-} depending upon the pH and the Cr(VI) concentration, the effect of these two parameters on the cyclic voltammetry (CV) and differential pulse voltammetry (DPV) responses was also investigated. In order to utilize the ion transfer reaction across the microhole array interface for the selective and sensitive detection of Cr(VI) ions, the assisted transfer of $HCrO_4^-$ anion by an Aliquat 336 ionophore incorporated into the PVC-NPOE gel phase was investigated using CV and differential pulse stripping voltammetry (DPSV). An excellent detection limit of 0.5 μM (26 ppb) with a wide linear dynamic range extending from 0.5 μM to 10 μM was achieved.

1. Introduction

The analysis of various chromium species is of immense importance due to their interesting physicochemical properties as well as their significant impact in environment and biochemical activity in human body. With several oxidation states possible for chromium, the two most common states present in an ambient environment are the Cr(III) and Cr(VI) ions. Trivalent chromium is considered as an essential trace element responsible for glucose and cholesterol metabolism in humans and other animals [1]. The Cr(VI) ion is known as a human respiratory carcinogen and is associated with various skin diseases such as skin allergies, dermatitis, dermal necrosis and dermal corrosion [2,3]. Moreover, Cr(VI) ions have been reported to be 100–1000 times more toxic than Cr(III) ions [4] and the World Health Organization (WHO) has thus recommended a provisional upper limiting value of 0.05 mg L^{-1} (50 ppb) in groundwater [5,6]. Considering the different toxicities of the two valence states of Cr, rather than the total concentration of Cr, the development of a fast and sensitive detection method specific to Cr(VI) ions in environmental samples could be powerfully employed to accurately assess pollution levels and help prevent further environmental contamination in industrial zones.

Several methods have been introduced for the successful detection and quantification of Cr(VI) in an aqueous phase such as atomic absorption spectrophotometry [7,8], high pressure liquid chromatography [9,10], X-ray fluorescence [11], inductively coupled plasma emission spectrometry [12] and optical sensors [13]. Although these methods offer reliable, accurate and reproducible analysis, some drawbacks remain such as being time-consuming, requiring sample pretreatment, high instrumentation costs as well as difficulty in clearly differentiating between different oxidation states [13]. Alternatively, electrochemical methods have attracted interest for Cr(VI) detection due to rapid and accurate analyses, great potentials for miniaturization as well as high sensitivities and selectivities [14]. A wide spectrum of solid metal electrodes [15], modified solid electrodes [16], gold and silver

* Corresponding author.
E-mail addresses: hyejinlee@knu.ac.kr, leehyejin82@gmail.com (H.J. Lee).

0013-4686/$ – see front matter © 2012 Elsevier Ltd. All rights reserved.
http://dx.doi.org/10.1016/j.electacta.2012.03.127

nanoparticles [17–19] combined electrodes have been investigated for trace Cr(VI) ion analysis. An alternative to commonly applied solid electrode based electrochemical techniques is the use of ion transfer reactions across a polarized interface between two immiscible electrolyte solutions (ITIES). The measurement of current associated with an ion transfer reaction at a liquid/liquid interface has been implemented as a sensitive and selective detection platform for various ionic species [20] and heavy metal ions [21]. However, Cr(VI) ions in a water environment form various hydrophilic anionic species such as $Cr_2O_7^{2-}$, $HCrO_4^-$, and CrO_4^{2-} which usually require a high Gibbs energies of transfer and makes it difficult to implement the ITIES as a sensing tool.

There have thus been only a few reports to date investigating hydrophilic anion transfer across a liquid/liquid interface and the subsequent creation of sensors [22,23]. For instance, Girault et al., reported the use of an ionic liquid composed of a highly hydrophobic supporting electrolyte which enables a wider potential window at more negative values [24] for the studies of I^-, Br^- and Cl^- anions. O'Mahony et al., demonstrated Cr(VI) ion transfer voltammetry in the form of $HCrO_4^-$ across the water/1,2-dichloroethane and the water/1,6-dichlorohexane interface using a polyamine macrocycle 2,5,8,11,14-pentaaza[15]-16,29-phenanthrolinophane as a Cr(VI) selective ionophore [25]. The use of the ionophore was to enhance the selectivity of Cr(VI) sensing and also to lower the Gibbs transfer energy of Cr(VI) ions across the liquid/liquid interface. However, a practical limitation of utilizing a large liquid/liquid interface (about 1 cm^2) as a sensing platform is mainly the mechanical instability and uncompensated ohmic loss due to the highly resistive organic phase [20]. To avoid these problems we have recently demonstrated the use of a micro-liquid/gel interface featuring a microhole or a microhole array interface supported on a thin polymeric film in conjunction with a gelified organic phase [20,26].

In this paper, the transfer reaction of various hexachromic anions across a 66 microhole array-liquid/PVC-NPOE gel interface with a hydrophobic organic supporting electrolyte was investigated using voltammetric methods. TOA^+ ions from the tetraoctylammonium tetrakis (pentafluorophenyl)borate (TOATB) organic supporting electrolyte having a relatively high Gibbs energy of transfer provides an extended potential window at the negative end and thus allows us to characterize the voltammetric responses due to the transfer of hydrophilic hexachromic anion species across a liquid/gel interface. The effect of pH of the aqueous phase and the concentration of Cr(VI) ions on the formation of different hexachromic anion species was studied using both cyclic voltammetry (CV) and differential pulse voltammetry (DPV). Moreover, a facilitated transfer of Cr(VI) in the form of $HCrO_4^-$ by a Cr(VI) selective ionophore, Aliquat 336 incorporated in the PVC-NPOE gel phase was developed for the selective and sensitive detection of Cr(VI) in conjunction with differential pulse stripping voltammetry (DPSV).

2. Experimental

2.1. Reagents

Polyvinylchloride (PVC, high molecular weight, Sigma–Aldrich), 2-nitrophenyloctylether (NPOE, Fluka), tricaprylmethylammonium chloride (Aliquat 336, Sigma–Aldrich), sodium chloride (NaCl, Merck), potassium chloride (KCl, Merck), potassium dichromate ($K_2Cr_2O_7$, Sigma–Aldrich), tetramethylammonium chloride (TMACl, >97%, Sigma–Aldrich), sodium sulfate (Na_2SO_4, Shinyo Pure Chem. Ind. Ltd.), potassium sulfate (K_2SO_4, Sigma–Aldrich), sodium acetate (CH_3COONa, Sigma–Aldrich), sodium bicarbonate ($NaHCO_3$, Sigma–Aldrich), sodium nitrate ($NaNO_3$, Sigma–Aldrich), sodium iodide (NaI, Sigma–Aldrich), sodium thiocyanate (NaSCN, Sigma–Aldrich), lithium tetrakis(pentafluorophenyl)-borate etherate (LiTB, Boulder Scientific Company), tetraoctylammonium bromide (TOABr, Fluka), tetraoctylammonium chloride (TOACl, Sigma–Aldrich) were all used as received. The organic phase supporting electrolyte, tetraoctylammonium tetrakis(pentafluorophenyl)borate (TOATB) was prepared by metathesis 1:1 of tetraoctylammonium bromide (TOABr) and lithium tetrakis(pentafluorophenyl)-borate etherate (LiTB) in methanol and water (v/v = 2:1) mixtures. The resulting precipitates were separated from the reaction mixtures by filtration followed by the several washing steps with Millipore-filtered water. The solvent was then evaporated using a vacuum dryer at 100 °C overnight. All aqueous solutions were prepared using Millipore-filtered water. The pH of the aqueous solution was adjusted by adding either diluted NaOH or H_2SO_4 to the Millipore-filtered water. Note that caution is required for adjusting the pH of the aqueous solution as the presence of chromate can also alter the pH of the prepared aqueous solution.

2.2. Fabrication of microhole array-liquid/gel interface

An array of 66 (11 × 6) microholes on a polyethylene terephthalate film (PET, 12 μm thick, Melinex type 'S' from ICI Films, UK) which serves as the interface for the water/organic gel layer was fabricated via photoablation using a UV Excimer laser according to the procedure described previously [27]. The diameter of each microhole was determined as 22 μm and 13 μm for the entrance and exit sides respectively. Prior to the gelification of the organic layer, PVC (3.0% w/w) and 10 mM TOATB were first dissolved in NPOE at 120 °C for 30 min. A twelve microliter of the PVC-NPOE mixture at 80 °C was then casted on the exit side of the 66 microhole array on the PET film and kept for a minimum of 6 h at room temperature to cool down and form a gelified layer.

2.3. Electrochemical measurements

All electrochemical experiments were conducted in a two-electrode mode using a computer-controlled potentiostat (Autolab PGSTAT30 Ecochemie) without any IR drop compensation. General Purpose Electrochemical System (GPES) version software v.4.9 was used to acquire and analyze the electrochemical data. All experiments were carried out at room temperature and the scan rate for cyclic voltammetry experiments was 20 mV s^{-1} unless otherwise stated.

3. Results and discussion

3.1. Voltammetric characterization of hexachromic anion transfer reaction across a microhole array water/gel interface

The direct transfer reactions of hexachromic anions across the microhole array interface between water and a PVC-NPOE gel layer incorporating TOATB as an organic supporting electrolyte were first studied using cyclic voltammetry. The role of TOATB was to provide a wider potential window to characterize the voltammetric response of hydrophilic hexachromic anions which could limit the negative end potential. A simplified predominance diagram shown in Fig. 1 inset is adopted from previous studies [5,28] in accordance with our experimental data. The previous literature [5,28] revealed that the hexavalent chromium shows different anionic forms in the aqueous phase depending on the solution pH and Cr(VI) concentration. At a low pH range (0.75–6.45) two dominant species of Cr(VI) exist in aqueous solution; $HCrO_4^-$ is the dominating species at lower concentrations (below 200 μM) and $Cr_2O_7^{2-}$ dominates at higher concentrations of Cr(VI). The dotted lines in the predominance diagram express the equilibrium point between the two species. For example, for the lower concentration

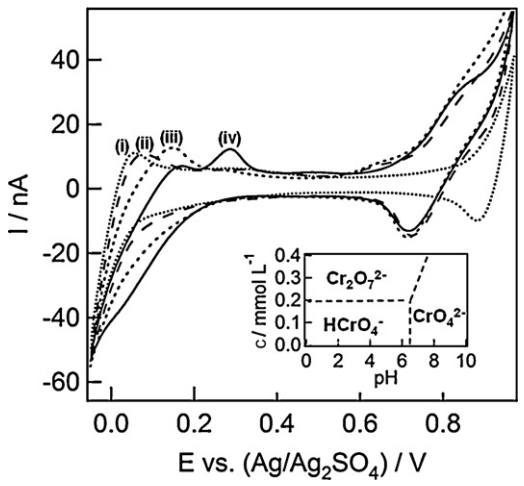

Fig. 1. Representative cyclic voltammograms showing the transfer of various hexachromic anionic species across the 66 microhole array interface between the aqueous and PVC-NPOE gel phase at different pH conditions in the presence of TMA^+ ions as an internal reference. (i) 10 mM Na_2SO_4 in the absence of Cr(VI) at pH 7. In the presence of 200 μM Cr(VI) at (ii) pH 10, (iii) pH 7 and (iv) pH 4. Cell 1 is used with 10 mM Na_2SO_4 and 100 μM TMACl. Scan rate is 20 mV s^{-1}. Inset shows a simplified predominance diagram for the various anionic species of Cr(VI) as a function of the pH and the total Cr(VI) concentration.

of Cr(VI) the dotted line at pH 6.45 indicates the equilibrium point between $HCrO_4^-$ and CrO_4^{2-}. Above this pH, $HCrO_4^-$ ions decrease while CrO_4^{2-} ions become dominating and vice versa for below pH 6.45. Therefore, our initial experiments were focused on monitoring the interfacial transfer of different Cr(VI) anions at various pH values while maintaining a fixed Cr(VI) concentration of 200 μM. The voltammetric measurements were performed in the presence of an internal reference, 100 μM TMA^+ ion, using the electrochemical cell set-up described in Cell 1.

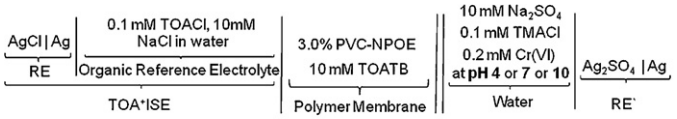

Cell 1

Cyclic voltammograms associated with the transfer of various hexachromic anions from the aqueous to the organic gel phases are displayed in Fig. 1. In the absence of Cr(VI) and TMA^+ ions, the positive end of the potential window is set by the transfer of Na^+ or TB^- ions, while the negative end is limited by the transfer of either TOA^+ or SO_4^{2-} ions across the micro-water/PVC-NPOE gel interface (see Fig. 1(i)). In the presence of both 100 μM TMA^+ ions and 200 μM Cr(VI) ions in the aqueous solution at pH values of 10, 7 and 4 (see Fig. 1(ii)–(iv)), two distinctive features are noticeable. Firstly, as the voltage is scanned in a positive (forward) direction, a steady-state current is obtained with a peak-shaped voltammogram observed on the reverse scan due to the transfer of TMA^+ ions across the interface within the available potential window. This asymmetric voltammogram shape is a unique characteristic associated with asymmetric diffusion regimes when using the microhole array interface between the water and PVC-NPOE gel phases. When TMA^+ ions transfer from the aqueous to the organic phase, a hemispherical diffusion flux similar to that obtained on solid microdisc electrodes dominates the steady-state current. Whereas for the transfer back of TMA^+ ions from the organic to the aqueous phase, a linear diffusion flux dominates due to the resistive holes present in the gel and resulting in a current peak formation [27,29]. When comparing results at different pH values, no significant variation in the steady-state and peak current responses was observed. This clearly indicates that TMA^+ ion transfer is independent of pH variation. Secondly, as the potential was scanned towards more negative values, the transfer of Cr(VI) ions having different anionic forms such as $Cr_2O_7^{2-}$, $HCrO_4^-$, and CrO_4^{2-} across the water/organic gel interface was observed. The appearance of different peaks and steady-state voltammetric responses at different potentials is indicative of more than one hexachromic species present in the aqueous solution. The experiments were performed using different sets of microhole water/gel interfaces which exhibit slight variations of ±15 mV potential window when compared. This was also observed in our previous studies involving the microhole water/organic gel interface [20]. Additional data is presented in the Supporting Information for the transfer reaction of 0.05 mM and 0.1 mM TMA^+ ions across micro-water/gel interfaces at pH values of 4, 7 and 10 in the presence of 10 mM Na_2SO_4.

The CV in Fig. 1 labeled (ii) obtained at pH 10 shows a very slight increment of the steady-state current in the presence of 200 μM Cr(VI) compared to the CV in Fig. 1 (iii) showing a larger increment of the steady-state current and the peak current observed at pH 7 for the same concentration of Cr(VI). This indicates that the transfer reaction of the dominating anionic species of Cr(VI) in the basic pH medium is not visualized within the available potential window, indicating that it may not be the same species as that in the neutral pH. On the other hand, at the neutral pH medium a transferable Cr(VI) anionic species across the interface is present in the aqueous phase which leads to the increment of both the steady-state and the peak currents (Fig. 1(iii)). The most prominent amperometric signals for both the forward and backward scans for the same concentration (200 μM) of Cr(VI) were observed at pH 4 (see Fig. 1(iv)) compared to those for the pH 7 and 10 solutions. Interestingly, two significant returning peaks at 175 mV and 325 mV were observed at the acidic pH which corresponds to the presence of two different Cr(VI) anionic species. The differences between hexachromic anions transferring across the polarized 66 microhole array liquid/gel interface were further studied by varying the Cr(VI) concentration and the solution pH.

The distribution of various hexavalent chromium species in aqueous solution can be described by the following equilibrium reactions [30]:

$$H_2CrO_4 \leftrightarrow H^+ + \mathbf{HCrO_4^-} \quad (K_1 = 1.21) \tag{1}$$

$$HCrO_4^- \leftrightarrow H^+ + \mathbf{CrO_4^{2-}} \quad (K_2 = 3 \times 10^{-7}) \tag{2}$$

$$2HCrO_4^- \leftrightarrow \mathbf{Cr_2O_7^{2-}} + H_2O \quad (K_3 = 35.5) \tag{3}$$

$$HCr_2O_7^- \leftrightarrow H^+ + \mathbf{Cr_2O_7^{2-}} \quad (K_4 = 0.85) \tag{4}$$

This suggests that Cr(VI) ions exist as CrO_4^{2-}, $Cr_2O_7^{2-}$, $HCrO_4^-$ and $HCr_2O_7^-$ in the aqueous phase depending on the pH of the aqueous solution and the total Cr(VI) concentration [5,13,28,31]. In order to design a Cr(VI) sensitive sensor selectively responding to a single type of Cr(VI) species, we initially focused on studying the transfer reactions of Cr(VI) anionic species across the polarized microhole liquid/gel interface at three different aqueous solution pH values of 4, 7 and 10 in addition to varying the concentration of Cr(VI) in aqueous phase using Cell 2.

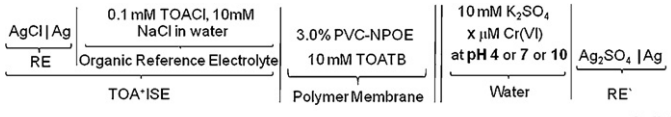

Cell 2

Fig. 2 shows a series of cyclic voltammograms for the transfer of hexachromic anions at concentrations of 50, 100 and 150 μM across the micro-aqueous/PVC-NPOE gel interface at an aqueous solution pH of 4 using Cell 2. In the absence of Cr(VI), the potential window was set by either K^+ or TB^- ion transfer at the positive end and by either SO_4^{2-} or TOA^+ ion transfer at the negative end. Following

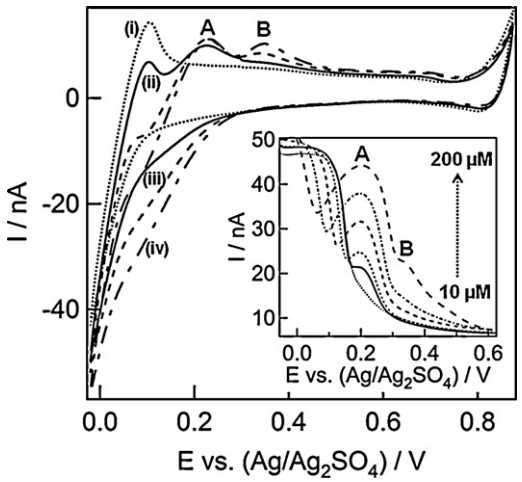

Fig. 2. A series of cyclic voltammograms for different concentrations of Cr(VI) ions transferring across a micro-aqueous/PVC-NPOE gel interface at a fixed aqueous solution pH of 4 using Cell 2. (i) 10 mM K_2SO_4 in the absence of Cr(VI) ions as well as (ii) 50 μM, (iii) 100 μM and (iv) 150 μM Cr(VI) ions. Scan rate = 20 mV s^{-1}. Inset shows differential pulse voltammograms obtained for the sensing of Cr(VI) at concentrations of 0, 10, 20, 50, 100 and 200 μM. The scan is directed from a low to high positive potential to drive the hexachromic anion transfer from the PVC-NPOE gel layer to the aqueous phase without applying a preconcentration step. Potential increment = 10 mV, pulse potential = 50 mV and pulse duration = 50 ms.

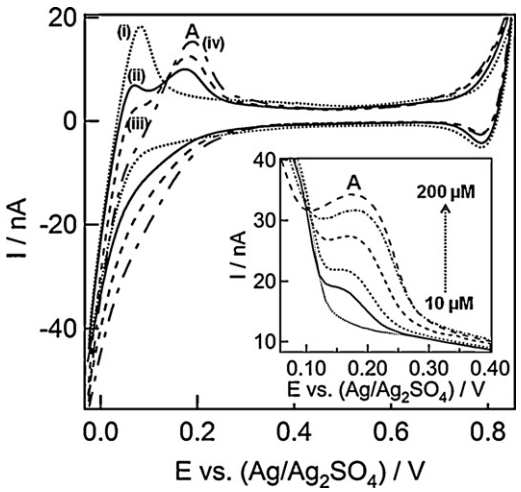

Fig. 3. Cyclic voltammograms for different concentrations of Cr(VI) ions transferring across a microhole-water/PVC-NPOE gel interface at an aqueous solution pH of 7 using Cell 2. (i) 10 mM K_2SO_4 in the absence of Cr(VI) and (ii) 50 μM, (iii) 200 μM and (iv) 400 μM Cr(VI) ions. Scan rate = 20 mV s^{-1}. Inset shows differential pulse voltammograms for the detection of Cr(VI) transferring back from the organic gel layer to the aqueous phase. Cr(VI) concentrations are 0, 10, 20, 50, 100 and 200 μM. All other DPV parameters are the same as in Fig. 2.

the addition of Cr(VI) in the aqueous phase, a steady-state current on the forward scan was observed due to the hemi-spherical diffusion of hexachromic anions from the aqueous to the organic phase, while a peak-shaped voltammogram on the reverse scan was observed mainly due to the mixture of a linear (in the microhole region filled with the gel) and a hemi-spherical (in the gel) diffusion flux of hexachromic anions transferring from the organic gel to the aqueous phase. The steady-state current increased linearly as a function of Cr(VI) concentration, while two distinctive peak currents responsible for the Cr(VI) transferring back from the organic to the aqueous phase were observed and whose current intensities varied with Cr(VI) concentration. The first peak current at 200 mV (A) increased linearly up to 100 μM Cr(VI) and did not increase any further when the Cr(VI) concentration increased to 150 μM. The second peak current at 350 mV (B) increased with respect to increments in the Cr(VI) concentration from 50 μM to 150 μM. At 150 μM Cr(VI), the two peak (A and B) current values became equal.

Considering that the predominant Cr(VI) anionic species in the range $6 \geq pH \geq 2$ is $HCrO_4^-$ at lower concentrations of Cr(VI) (< 190 μM) while the $Cr_2O_7^{2-}$ anion prevails at higher concentrations (>190 μM) [5,13], the first peak A showing a higher current in the concentration range of 50–100 μM was assigned to the transfer of $HCrO_4^-$, while the second peak B is associated with the transfer of $Cr_2O_7^{2-}$. For 150 μM of Cr(VI), peak A responsible for the transfer of $HCrO_4^-$ and the peak B responsible for the transfer of $Cr_2O_7^{2-}$ are equal. Therefore, we can consider this as an equilibrium concentration point for both phases. This observation was further verified using differential pulse voltammetry (DPV) with the same cell set-up where the scan was directed from a low to a high positive potential to drive the transfer of different concentrations of hexachromic anions back from the PVC-NPOE gel layer to the aqueous phase without applying any preconcentration step. DPV parameters used are the potential increment of 10 mV, the pulse potential of 50 mV and the pulse duration of 50 ms. The DPV's in the Fig. 2 inset show that the first peak A (related to the transfer of $HCrO_4^-$) linearly increased with increasing Cr(VI) concentrations up to 200 μM, while peak B (i.e., $Cr_2O_7^{2-}$ transfer) appeared above 100 μM and became prominent around 200 μM Cr(VI) ions. Note that peak B decreases significantly below 100 μM, which can be more distinctively observed in the Fig. 2 inset compared to the cyclic voltammograms in Fig. 2. This may be due to overlapping of peak B at 350 mV with a significant capacitive current that appears in the region between 100 mV and 600 mV and which can be experimentally observed. The capacitive current may be due to a possible interfacial charging effect caused by the repeated transfer processes of ionic species including the aqueous supporting electrolytes coming from consecutive runs of Cr(VI) analysis using the same microarray-water/gel interface. We found the equilibrium concentration point of $HCrO_4^-$ and $Cr_2O_7^{2-}$ anions to be in the range of 150–200 μM, which is in good agreement with the previously reported value of about 190 μM [5,13]. It can thus be concluded that the two most favoured hexachromic anion species of $HCrO_4^-$ and $Cr_2O_7^{2-}$ are present in the aqueous solution at pH 4 and that this statement is supported by the literature [2,5,28].

Cyclic voltammograms and differential pulse voltammograms obtained using Cell 2 for Cr(VI) concentrations ranging from 10 to 400 μM at an aqueous solution pH of 7 are presented in Fig. 3. The CVs show that both the steady-state and the peak current increased as the Cr(VI) concentration increased. Only one peak A at 200 mV appeared and the peak current increased linearly up to 400 μM which can be associated with the $HCrO_4^-$ ion transferring from the organic gel to the aqueous phase. The predominance diagram presented in Fig. 1 (inset) [5] suggests that the $HCrO_4^-$ ion is the predominant species for the pH range of 0.75–6.45. However, $HCrO_4^-$ ions also exist in aqueous solution at neutral conditions (pH 7) in slightly lower concentrations than that at the equilibrium point, which was also reported by Brito et al. [28]. Also the increment of the peak A current at pH 7 was relatively lower than that of the pH 4. In addition, comparing both the DPV data at pH 7 (Fig. 3, inset) and at pH 4 (Fig. 2, inset), the potential where peak A appears at pH 7 is overlapping with the potential for the peak A position at pH 4, which indicates that the dominating Cr(VI) species transferring across the interface is $HCrO_4^-$ at pH 7.

The voltammetric responses for the transfer of Cr(VI) concentrations ranging from 20 μM to 400 μM at the aqueous solution pH of 10 are shown in Fig. 4 with negligible increases in signal observed upon increasing the Cr(VI) concentration. At this basic condition (above pH 8) the main species present is known to be CrO_4^{2-} [28], of which the transfer process is not realized within the available

potential window due to its relatively high Gibbs energy to charge ratio of transfer required across the water/gel interface. However, a small change in the DPVs response (Fig. 4, inset) was observed at a concentration of 100 μM, which may come from the presence of a very small fraction of $HCrO_4^-$ at pH 10. The summary of results shown in Figs. 1–4 is represented as a simplified predominance diagram representing the relative distribution of various hexachromic anions in an aqueous phase (see Fig. 1, inset). Overall, two different hexachromic anions, $HCrO_4^-$ and $Cr_2O_7^{2-}$ predominantly exist in the acidic aqueous solution (pH 4), while $HCrO_4^-$ becomes the dominating species as the solution pH condition becomes neutral and the CrO_4^{2-} anion is the dominating species at even higher pH's for the Cr(VI) concentration ranging from 10 μM to 400 μM.

3.2. Cr(VI) selective sensors with the facilitated transfer of $HCrO_4^-$ by Aliquat 336 across micro-liquid/gel interface

Since the maximum concentration of Cr(VI) ions in ground water recommended by the WHO is 50 ppb (0.96 μM) [5,6], our aim was to detect Cr(VI) species at low ppb concentrations in the aqueous phase. The voltammetric studies described above established that at both lower pH ($6 \geq pH \geq 2$) and concentration values (<200 μM), $HCrO_4^-$ is the dominating species transferring across micro-liquid/gel interface within the available potential window when using TOATB and K_2SO_4 supporting electrolytes. Therefore, we designed our experiment to operate at pH 4 to improve the detectability of a μM concentration range of Cr(VI) in the form of $HCrO_4^-$ using differential pulse stripping voltammetry (DPSV) in conjunction with the incorporation of a highly $HCrO_4^-$ selective ionophore in the organic phase to enhance the selectivity of our sensing platform. Among the various available ionophores, the quaternary ammonium salt, Aliquat 336 was chosen to assist the selective transfer of $HCrO_4^-$ across the polarized microhole interface since this has been reported as a highly selective carrier for $HCrO_4^-$ [32,33] and utilized in different electrochemical [31,34] and optical [13] systems. A concentration of 10 mM Aliquat 336 was introduced to the PVC-NPOE organic gel containing 10 mM TOATB as an organic supporting electrolyte and the assisted transfer characteristics of Cr(VI) by the ionophore across the liquid/gel interface were studied using cyclic voltammetry and Cell 3.

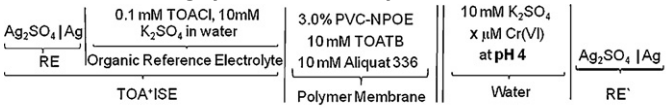

Cell 3

Fig. 5 represents a series of cyclic voltammograms for various concentrations of Cr(VI) transferring from the aqueous to the organic phase and vice versa across the polarized microhole-water/PVC-NPOE gel interface. In the absence of Cr(VI) (Fig. 5(i)), no steady-state current was observed within the given potential window. Upon the addition of Cr(VI) to the aqueous phase, a steady-state current on the forward scan was observed. This is associated with the transfer of $HCrO_4^-$ ions facilitated by Aliquat 336 from the aqueous to the organic phase. On the reverse scan, a peak was observed due to $HCrO_4^-$ ions transferring back from the organic gel to the aqueous phase. The same asymmetric voltammetric responses were achieved as in the case of the direct $HCrO_4^-$ ion transfer due to the asymmetric diffusion flux across the aqueous/gel interface. At a concentration of 25 μM, two peaks on the reverse scan appeared (Fig. 5(ii)) and upon increasing the concentration from 25 μM up to 100 μM, the peak A at 300 mV also significantly increased (Fig. 5(iii) and (iv)). Taking into consideration the direct ion transfer data in Fig. 2 (inset) along with previous literature [5,13] and also that Aliquat 336 selectively interacts only monovalent oxyanions, i.e., $HCrO_4^-$ [32], it can be concluded that the peak A is due to the assisted transfer of $HCrO_4^-$ by Aliquat 336.

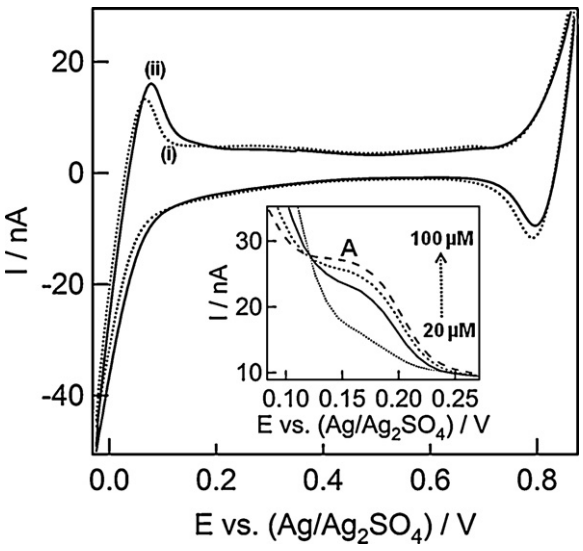

Fig. 4. Cyclic voltammograms for Cr(VI) ions transferring across a micro-water/PVC-NPOE gel interface at a fixed aqueous solution pH of 10 using Cell 2. (i) 10 mM K_2SO_4 in the absence of Cr(VI) and (ii) 400 μM Cr(VI) ions. Scan rate = 20 mV s^{-1}. Inset shows differential pulse voltammograms obtained for the sensing of Cr(VI) at concentrations of 0, 20, 50 and 100 μM. All other DPV parameters are the same as in Fig. 2.

The appearance of peak A at a slightly more positive potential than that associated with direct transfer is due to the fact that the facilitated transfer of $HCrO_4^-$ by the selective complexation with Aliquat 336 reduces the Gibbs energy of $HCrO_4^-$ transfer across the aqueous/organic gel interface. The steady-state current as well as the peak A current increased as a function of Cr(VI) concentration ranging from 5 μM to 100 μM with a minimum detection limit of about 5 μM of Cr(VI) at a signal to noise ratio of 3:1.

As a final demonstration, the use of differential pulse stripping voltammetry (DPSV) was investigated in an effort to further improve the Cr(VI) detection limit in conjunction with a

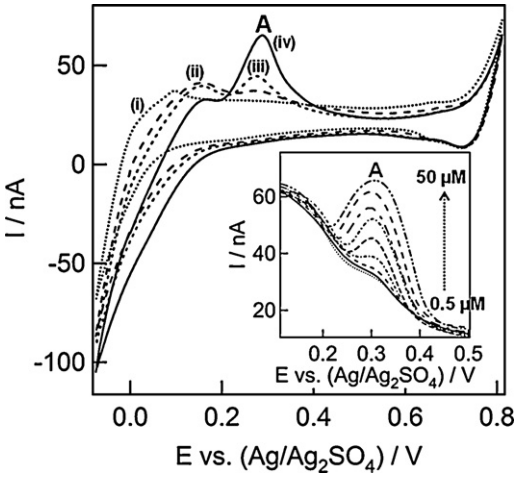

Fig. 5. A series of cyclic voltammograms for the assisted transfer of various concentrations of Cr(VI) ions across the micro-water/organic gel interface by Aliquat 336 present in the PVC-NPOE gel at a fixed aqueous solution pH of 4 using Cell 3. (i) 10 mM K_2SO_4 in the absence of Cr(VI) and (ii) 25 μM, (iii) 50 μM and (iv) 100 μM Cr(VI) ions. 10 mM Aliquat 336 is used and scan rate is 20 mV s^{-1}. Inset shows differential pulse stripping voltammograms for the detection of Cr(VI) ion concentrations ranging from 0, 0.5, 2, 5, 10, 20, 30, 40–50 μM. The scan is directed from a low to high positive potential to drive the $HCrO_4^-$ transfer from the PVC-NPOE gel layer to the aqueous phase. A deposition potential of 300 mV for 40 s prior to DPSV is applied for preconcentrating Cr(VI) ions in the organic phase. Potential increment = 10 mV, pulse potential = 50 mV and pulse duration = 50 ms.

Table 1
Amperometric selectivity coefficients of Cr(VI) selective sensors over various interfering anionic species.

Interfering anion	SCN^-	I^-	NO_3^-	Cl^-	NO_2^-	HCO_3^-	CH_3COO^-	SO_4^{2-}
$\log k_{i,j}^{amp}$	−1.39	−2.59	−2.85	−3.03	−3.16	*n.i.*	*n.i.*	*n.i.*

n.i.: not interfering.
i and *j* are the analyte (e.g., $HCrO_4^-$) and the interfering anion, respectively.

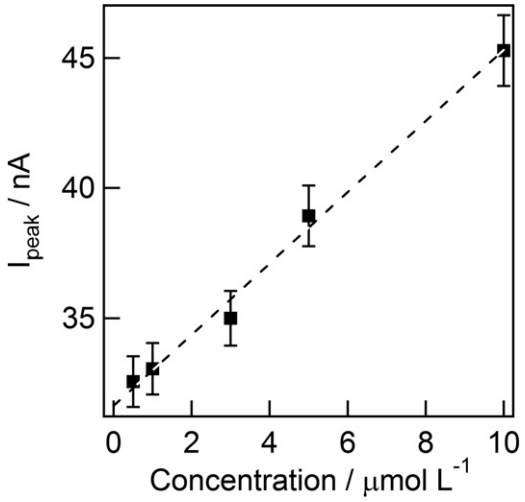

Fig. 6. A plot of the peak current value from the DPSV data in Fig. 5 versus the Cr(VI) concentration from 0.5 to 10 μM. The dotted line represents a linear fit.

preconcentration step which accumulates $HCrO_4^-$ anions in the organic gel layer. This was performed by first applying a positive potential of 300 mV for 40 s where the anion transfers from the aqueous to organic gel phase. The preconcentrated Cr(VI) ions were then stripped from the organic gel layer to the aqueous phase by scanning the potential from −50 mV to 650 mV with a potential step of 10 mV s^{-1}. Fig. 5 (inset) represents a series of differential pulse stripping voltammograms showing the increased stripping peak current as a function of the Cr(VI) concentration. From the plot of the DPSV peak current versus the Cr(VI) concentration in Fig. 6, a linear fit with a slope of 1.37 nA μM^{-1} for the Cr(VI) concentration ranging from 0.5 μM to 10 μM (26–520 ppb) was obtained. An excellent detection limit of 0.5 μM using a signal to noise ratio of 3:1 was established, which comfortably exceeds the requirements for detecting Cr(VI) in environmental samples (e.g., the current allowance is 50 ppb in ground water) [5,6].

An extension to real-field applicability was preliminarily investigated by determining the selectivity of the developed Cr(VI) sensor over various interfering anionic species. The amperometric selectivity coefficient was calculated using the fixed analyte concentration method according to the following equation [35].

$$k_{i,j}^{amp} = \frac{(I_t - I_i)C_i}{I_i C_j} \quad (5)$$

where, *i* and *j* are the analyte and the interfering agent, respectively and I_t is the total current from both the analyte and interfering agent. A series of experiments involving the Cr(VI) selectivity over various interfering agents including NO_3^-, I^-, SCN^- SO_4^{2-}, NO_2^-, CH_3COO^-, HCO_3^- and Cl^- were investigated. Each of the interfering agents, ranging in concentration from 0.01 mM to 1 mM, was added to the fixed analyte solution of 10 μM Cr(VI). The amperometric selectivity coefficient for our Cr(VI) sensor is listed in Table 1. NO_3^-, I^- and SCN^- anions have a relatively low interfering effect on the detection signal, which is much less than those of other Aliquat 336 based Cr(VI) selective electrochemical [34] or optical sensors [13]. More importantly, the sensing responses for Cr(VI) species exhibited a negligible interference up to a 100-fold excess of each interfering anions including SO_4^{2-}, NO_2^-, CH_3COO^-, HCO_3^- and Cl^- compared to the Cr(VI) ions. Each of these interferants is commonly present in natural water.

4. Conclusions

The voltammetric characteristics of various hexachromic anions transferring across a polarized 66 microhole array interface between the aqueous and PVC-NPOE gel phase incorporating TOATB organic supporting electrolyte in the gel layer were studied. Cr(VI) exists as a hydrophilic anionic species with different oxidative states in aqueous solution, which usually requires a highly negative potential to drive their transfer across a polarized water/PVC-NPOE gel interface. In order to fully characterize the voltammetric characteristics associated with the transfer of such hydrophilic hexachromic anions across the micro-water/gel interface, a newly synthesized TOATB salt providing a wider potential window at the negative end was synthesized and utilized. Both the pH of the aqueous analyte solution and the Cr(VI) concentration significantly affect the voltammetric responses of the Cr(VI) ion transfer reaction reflecting the varied anionic forms of Cr(VI) ions. By tailoring both these parameters, we demonstrated that at an analyte solution pH of 4, the Aliquat 336 facilitated transfer reaction of $HCrO_4^-$ ions across the micro-liquid/gel interface is a very sensitive and selective platform for Cr(VI) sensing. A detection limit of 0.5 μM (26 ppb) was achieved, which is about 10–40 times lower than those of other ionophore-based electrochemical sensors and optical sensors [13,25,34] in addition to a wide linearity ranging from 0.5 μM to 10 μM. Moreover, very good selectivity towards Cr(VI) was achieved against a wide range of anionic species commonly present in natural water samples. We envision that the developed amperometric Cr(VI) selective sensors with DPSV can be usefully implemented in a portable device for on-site investigations involving Cr(VI) ion pollutant monitoring in ground water.

Acknowledgements

This work was supported by the New & Renewable Energy of the Korea Institute of Energy Technology Evaluation and Planning (KETEP) grant funded by the Korea government Ministry of Knowledge Economy (No. 20093020030020-11-1-000) and National Research Foundation of Korea (20110004823).

Appendix A. Supplementary data

Supplementary data associated with this article can be found, in the online version, at http://dx.doi.org/10.1016/j.electacta.2012.03.127.

References

[1] M. Jakubowska, Journal of Hazardous Materials 176 (2010) 540.
[2] J. Kotaś, Z. Stasicka, Environmental Pollution 107 (2000) 263.
[3] J. Wang, K. Ashley, E.R. Kennedy, C. Neumeister, Analyst 122 (1997) 1307.
[4] R.M. Cespón-Romero, M.C. Yebra-Biurrun, M.P. Bermejo-Barrera, Analytica Chimica Acta 327 (1996) 37.
[5] C.M. Welch, O. Nekrassova, R.G. Compton, Talanta 65 (2005) 74.

[6] Guidance for Drinking Water Quality, Recommendations, vol. 1, 2nd ed., WHO, Geneva, 1993.
[7] J. Chwastowska, W. Skwara, E. Sterlińska, L. Pszonicki, Talanta 66 (2005) 1345.
[8] R.A. Gil, S. Cerutti, J.A. Gásquez, R.A. Olsina, L.D. Martinez, Talanta 68 (2006) 1065.
[9] Y. Martínez-Bravo, A.F. Roig-Navarro, F.J. López, F. Hernández, Journal of Chromatography A 926 (2001) 265.
[10] I. Ali, H.Y. Aboul-Enein, Chemosphere 48 (2002) 275.
[11] C. Fontàs, I. Queralt, M. Hidalgo, Spectrochimica Acta Part B 61 (2006) 407.
[12] A.E. Pillay, J.R. Williams, M.O. El Mardi, S.M.H. Al-Lawati, M.H. Al-Hadabbi, A. Al-Hamdi, Environment International 29 (2003) 541.
[13] R. Güell, C. Fontàs, V. Salvadó, E. Anticó, Analytica Chimica Acta 594 (2007) 162.
[14] N.A. Carrington, L. Yong, Z.-L. Xue, Analytica Chimica Acta 572 (2006) 17.
[15] L. Lin, N.S. Lawrence, S. Thongngamdee, J. Wang, Y. Lin, Talanta 65 (2005) 144.
[16] M.F. Bergamini, D.P. dos Santos, M.V.B. Zanoni, Sensors and Actuators B 123 (2007) 902.
[17] G. Liu, Y.-Y. Lin, H. Wu, Y. Lin, Environmental Science and Technology 41 (2007) 8129.
[18] O. Domínguez-Renedo, L. Ruiz-Espelt, N. García-Astorgano, M.J. Arcos-Martínez, Talanta 76 (2008) 854.
[19] B.K. Jena, C.R. Raj, Talanta 76 (2008) 161.
[20] H.J. Lee, C. Beriet, H.H. Girault, Journal of Electroanalytical Chemistry 453 (1998) 211.
[21] H.J. Lee, G. Lagger, C.M. Pereira, A.F. Silva, H.H. Girault, Talanta 78 (2009) 66.
[22] H.J. Lee, C.M. Pereira, A.F. Silva, H.H. Girault, Analytical Chemistry 72 (2000) 5562.
[23] B. Quinn, R. Lahtinen, L. Murtomäki, Journal of Electroanalytical Chemistry 460 (1999) 149.
[24] A.J. Olaya, M.A. Méndez, F. Cortes-Salazar, H.H. Girault, Journal of Electroanalytical Chemistry 644 (2010) 60.
[25] A.M. O'Mahony, M.D. Scanlon, A. Berduque, V. Beni, D.W.M. Arrigan, E. Faggi, A. Bencini, Electrochemistry Communications 7 (2005) 976.
[26] M.M. Hossain, S.N. Faisal, C.S. Kim, H.J. Cha, S.C. Nam, H.J. Lee, Electrochemistry Communications 13 (2011) 611.
[27] H.J. Lee, P.D. Beattie, B.J. Seddon, M.D. Osborne, H.H. Girault, Journal of Electroanalytical Chemistry 440 (1997) 73.
[28] F. Brito, J. Ascanio, S. Mateo, C. Hernández, L. Araujo, P. Gili, P. Martín-Zarza, S. Domínguez, A. Mederos, Polyhedron 16 (1997) 3835.
[29] S.N. Faisal, C.M. Pereira, S. Rho, H.J. Lee, Physical Chemistry Chemical Physics 12 (2010) 15184.
[30] N. Kabay, M. Arda, B. Saha, M. Streat, Reactive and Functional Polymers 54 (2003) 103.
[31] F. Kong, Y. Ni, BioResources 4 (2009) 1088.
[32] A. Bhowal, S. Datta, Journal of Membrane Science 188 (2001) 1.
[33] C.A. Kozlowski, W. Walkowiak, Journal of Membrane Science 266 (2005) 143.
[34] Y.-W. Choi, S.-H. Moon, Environmental Monitoring and Assessment 92 (2004) 163.
[35] C. Maccà, J. Wang, Analytica Chimica Acta 303 (1995) 265.